RECONSTRUCTION OF ELLIPSOIDS ON ROLLERS FROM STEREO IMAGES USING OCCLUDING CONTOURS

Sudanthi N.R. Wijewickrema and Andrew P. Papliński
Clayton School of Information Technology
Monash University, Victoria, 3800, Australia

Charles E. Esson
Colour Vision Systems Pty Ltd
11 Park Street, Bacchus Marsh, Victoria, 3340, Australia

Keywords: Quadric Reconstruction, Ellipsoid Modelling, Occluding Contours, Fruit Sorting.

Abstract: We describe the reconstruction of quadric surfaces with special attention on ellipsoids, using two different views from calibrated cameras, given that they rest on known objects in space. The technique proposed focuses basically on speed and efficiency and is suitable to be used in resource constrained environments in real time.

We model the quadric in dual space and introduce a method of including application specific information in the reconstruction. We also discuss a novel and fast way of adjusting the occluding contours to fit the epipolar tangency constraints before the reconstruction. We further apply this to a real-life application where ellipsoidal fruits are modelled in 3d. Then, we analyze the error of fit for the reconstructed quadrics. Although this paper focuses on ellipsoids, it can be easily extended to incorporate the modelling of other non-degenerate quadrics using two occluding contours in dual space.

1 INTRODUCTION

Reconstruction of quadric surfaces from occluding contours is essential when dealing with non-textured smooth surfaces where correspondence between features cannot be obtained. Early works of this kind include (Giblin and Weiss, 1987) where the profiles of a smooth surface was used in the reconstruction given that the motion of the camera was small, known and coplanar. Another approach to surface reconstruction was later developed that could incorporate large variations of camera motion between views (Ma and Li, 1996; Mendonca et al., 2000). These were further developed to include unknown camera motion (Cross et al., 1999; Mendonca et al., 2000).

(Ma and Chen, 1994) introduced a non-linear reconstruction method for quadrics using perspective views. (Ma and Li, 1996) builds on (Ma and Chen, 1994) and (Karl et al., 1994), which discusses the reconstruction of ellipsoid surfaces from the silhouettes of its orthographic projections. Both (Karl et al., 1994) and (Ma and Li, 1996) investigate the special case of reconstructing ellipsoids and the former shows how this can be done with three or more orthogonal views. The latter uses three perspective views and for calibrated cameras, it is a linear calculation.

Techniques such as (Cross and Zisserman, 1998) use the duality property of points and planes in the homogeneous coordinate system. (Cross, 2000) discusses 3d surface reconstruction in detail for single and multiple view cases and explains the use of occluding contours in dual space and/or additional points/planes in the calculation. (Kang et al., 2001; Kang et al., 2003) use occluding contours to calculate the tangent planes to the surface and perform the fitting of a dual quadric in the space of planes.

The aim of this paper is to discuss a method of quadric surface reconstruction using occluding contours of two perspective images focusing on the special case of ellipsoids. Among others, we build on the work of (Cross and Zisserman, 1998) and (Cross, 2000). The main focus of this algorithm is to maximize efficiency. Hence, it avoids non-linear iterative methods and searching techniques (e.g. finding correspondence). The desired application requires higher speed, that leads to resource constraints. The solutions obtained here are suitable for such an environment.

N. R. Wijewickrema S., P. Papliñki A. and E. Esson C. (2006).
RECONSTRUCTION OF ELLIPSOIDS ON ROLLERS FROM STEREO IMAGES USING OCCLUDING CONTOURS.
In *Proceedings of the First International Conference on Computer Vision Theory and Applications*, pages 370-376
DOI: 10.5220/0001366903700376

2 OVERVIEW

This section gives an overview of the method used in the quadric reconstruction and how the paper is structured. The algorithm uses images taken from two non-concentric, calibrated cameras, fits conics to them and reconstructs the quadric with the use of additional information. The technique can be summarized as follows:

- Fit conics to the projections (images)
- Align the two fitted conics so that they adhere to the epipolar geometry
- Reconstruct the family of quadrics in dual space
- Select a quadric that sits on one or more known quadric surfaces

The rest of the paper explains this method in detail. Section 3 discusses quadrics and the duality principle and then goes on to explain how the reconstruction is done in dual space. Section 4 discusses how to introduce application specific information into the calculation. Section 5 addresses the implementation specific problem of the conics not fitting epipolar tangency constraints. It introduces an algorithm to adjust them accordingly. Then, experimental results are given in Section 6 where the algorithm is applied to data obtained from fruit sorting applications.

3 QUADRICS AND DUAL SPACES

A quadric is a surface in 3d, represented by a 4×4 symmetric matrix Q. For each point $\mathbf{X}$ on the surface, represented by a homogeneous coordinate vector $\mathbf{X} = [x \;\; y \;\; z \;\; 1]^T$, the following condition should be satisfied.

$$\mathbf{X}^T Q \mathbf{X} = 0 \tag{1}$$

The pole-polar relationship for a quadric is defined as follows. If $\mathbf{X}$ is a point anywhere in space, then there exists a plane $\boldsymbol{\pi}$ satisfying the condition in eqn (2). Then, $\mathbf{X}$ is the pole and $\boldsymbol{\pi}$ is the corresponding polar plane with respect to the quadric Q. If the pole $\mathbf{X}$ lies on the surface of the quadric, the polar plane $\boldsymbol{\pi}$ becomes the tangent plane to the quadric at $\mathbf{X}$ (Hartley and Zisserman, 2003).

$$\boldsymbol{\pi} = Q\mathbf{X} \tag{2}$$

Duality in 3d is expressed as the interchangeability of points and planes (Bruce, 1992; Hartley and Zisserman, 2003). Considering the equation of a plane $\boldsymbol{\pi}^T\mathbf{X} = 0$, we can see that interchanging the 4 element vectors would not change the equation. So, by using eqns (1) and (2), we get the dual quadric Q^* which is defined by a set of planes and satisfies the constraint $\boldsymbol{\pi}^T Q^* \boldsymbol{\pi} = 0$.

$$Q^* = Q^{-1} \tag{3}$$

Alternatively, the dual can be defined as the adjoint of the quadric $Q^* = \text{adj}(Q)$ since $\text{adj}(Q) = \det(Q)Q^{-1}$ and the scale factor does not affect the quadric equation.

A conic can be defined in 2d space similar to a quadric by a 3×3 symmetric matrix, C. For a point in 2d $\mathbf{x}$ represented as a homogeneous vector of three elements lying on the conic, the constraint $\mathbf{x}^T C\mathbf{x} = 0$ is satisfied. The pole-polar relationship is similar to the case of a quadric where the pole is a point in 2d and the polar is a line. $\mathbf{l} = C\mathbf{x}$ gives the relationship between a pole and its polar line and if $\mathbf{x}$ is on C, the polar line is tangent to the conic. Duality between points and lines exists and a line conic can be defined as $C^* = C^{-1}$ or $C^* = \text{adj}(C)$ with $\mathbf{l}^T C^* \mathbf{l} = 0$

The outline of the projection of a quadric (*occluding contour*) is the projection of its *contour generator*. The contour generator is the curve formed by the tangency between the quadric and the cone of light rays leading to the camera center. Since the contour generator arises from tangency, it is more convenient to use the dual quadric of Q in the determination of the projected conic. Under the camera matrix P, the projection of the quadric Q is the conic C given by eqn (4). Here, Q^* and C^* are the duals of the quadric and the conic respectively. Proof of this can be found in (Hartley and Zisserman, 2003).

$$C^* = PQ^*P^T \tag{4}$$

A conic and a quadric have 5 and 9 degrees of freedom respectively. Hence, one projection of the quadric would impose 5 constraints on the reconstruction. In other words, the dual of the occluding contour conic defines 5 independent planes that the dual quadric has to be tangent to. In the case of two cameras though, epipolar tangency constraints dictate that the two tangent cones generated by the two cameras share two planes. Hence, in the case of two views only 8 constraints are imposed on the quadric. This indicates that given two views from two non-concentric cameras, we can obtain a family of dual quadrics as shown in eqn (5), where λ is a parameter and Q_1^* and Q_2^* are known. Details of this can be found in (Cross and Zisserman, 1998; Cross, 2000).

$$Q^*(\lambda) = Q_1^* + \lambda Q_2^* \tag{5}$$

4 TANGENCY INFORMATION

Section 3 explains the reconstruction of a family of quadrics. To remove the ambiguity, we need to introduce additional information such as another tangent plane or points on the surface. If point information is introduced, eqn (5) has to be inverted to get the family of quadrics in real space giving us a cubic equation in λ. Hence, solving the ambiguity in dual space is much simpler and more efficient.

We use the fact that most quadric surfaces in real life would rest on some known surface, be it a plane or another quadric in space. If the surface is a plane (say π_k), the unique quadric could be reconstructed easily by using $\pi_k^T Q^* \pi_k = 0$, giving us a value for λ as follows:

$$\lambda_k = -\frac{\pi_k^T Q_1^* \pi_k}{\pi_k^T Q_2^* \pi_k} \tag{6}$$

But in most situations, we might just know one or more other quadric surfaces that the quadric to be reconstructed is tangent to. We discuss a simple calculation to be used in such situations. For example, we consider a case where the quadric lies on a set of rollers (cylinders or cones).

In such cases, we use the fact that the quadric must rest on some plane parallel to the xy plane between a range of heights. The range of heights should be determined from the size and orientation of the known quadrics. For each of these heights, we calculate the plane π_k parallel to the xy plane and using eqn (6), get a unique dual quadric. Then for each of these dual quadrics, we check for tangency with one or more known quadrics in space. The following section describes how this is done in a fast and efficient manner.

4.1 Tangency Between Quadrics

Let the quadric to be reconstructed be Q_w and the known surface in space be Q_k. For the scope of this calculation, Q_k could be any non-degenerate or degenerate quadric while Q_w should be non-degenerate. Let $\mathbf{X}$ be any pole with respect to both quadrics and $\boldsymbol{\pi}$ be the respective polar plane. Then, the relationships in eqn (7) holds. Note that both equations give the same plane since the scale factor μ does not affect the equation of the plane.

$$\begin{aligned} \boldsymbol{\pi} &= \mu Q_w \mathbf{X} \\ \boldsymbol{\pi} &= Q_k \mathbf{X} \end{aligned} \tag{7}$$

$$(\mu Q_w - Qk)\mathbf{X} = 0 \implies (\mu I - P)\mathbf{X} = 0 \tag{8}$$

Where,

$P = Q_w^{-1} Q_k$ and I is the 4×4 identity matrix

This is an eigensystem which has four solutions that gives the common poles (values of $\mathbf{X}$) to the two quadrics Q_w and Q_k. By substituting them in eqn (7), we get the respective polar planes.

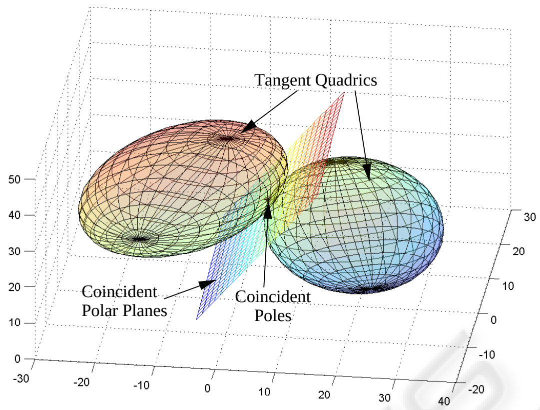

Figure 1: Tangent Quadrics and coinciding Poles/Polar Planes.

It was observed that if the quadrics are tangent to each other, out of these four solutions, two poles (and hence, the respective polar planes) coincide. In this case, the coincident poles lie on the surfaces of both Q_w and Q_k fulfilling the tangency requirement given in eqn (2). Figure 1 shows how two poles and polar planes coincide in a case of tangency.

5 CONIC ADJUSTMENT

To obtain the occluding contour of the projection, conics have to be fitted to the projected images. For this, any suitable conic fitting algorithm could be used. We use the ellipse specific algorithm discussed in (Wijewickrema and Papliński, 2005) as it is more suited for the type of application this is aimed for. It does not require edge detection (but only a simple segmentation of the object from the background) and uses a subset of points inside the object making it more robust against outliers.

In real applications, the fitted conics may not adhere to epipolar tangency constraints due to errors in fitting and the fact that the objects may not be ideal ellipsoids. Hence, a conic correction algorithm has to be applied on the fitted conics before the reconstruction. (Cross, 2000) discusses a method of non-linear optimization using the Levenberg-Marquardt method for this adjustment. Alternatively, we use a more efficient algorithm for conic adjustment using *frontier points* as discussed in the following section.

5.1 Frontier Points

The concept of *frontier points* was first introduced in (Rieger, 1986), and was interpreted in (Porril and Pollard, 1991) as the fixed point on the surface of the

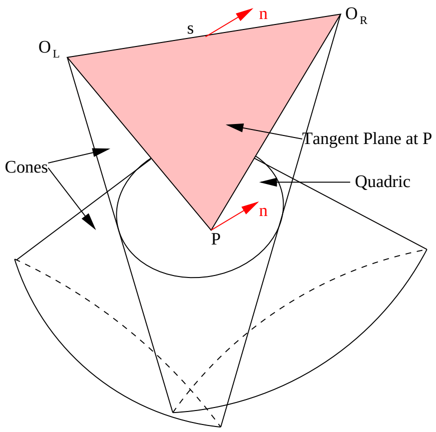

Figure 2: Tangent Plane at a Frontier Point.

quadric, corresponding to the intersection of two corresponding contour generators. Frontier points lie on the epipolar planes shared by the two tangent cones. This is explained in the *Occluding Edge Theorem* given in (Collins et al., 2004). It states that at the frontier points, the tangents to the two cones and the quadric coincide. Figure 2 shows this relationship. We further this theorem by using the following corollary.

Corollary 1: The tangent plane at a frontier point $\mathbf{P}$ to the cones and the quadric, contains the vector $\mathbf{s}$ joining the two cameras and the rays passing from either camera center to $\mathbf{P}$. Hence, the normal $\mathbf{n}$, to the tangent plane at $\mathbf{P}$ and $\mathbf{s}$ are orthogonal. That is:

$$\mathbf{s}^T\mathbf{n} = 0 \tag{9}$$

A cone is a degenerate quadric and hence could be represented using a 4×4 symmetric matrix that satisfies eqn (1). If it is represented by the matrix R, the normal $\mathbf{n}$ to the cone at a point $\mathbf{X}$ would be as shown in eqn (10), where $\bar{R}$ is a 3×4 matrix consisting of the first three rows of R.

$$\mathbf{n} = 2\bar{R}\mathbf{X} \tag{10}$$

Hence, at a frontier point $\mathbf{X}_f$, the normals $\mathbf{n}_L$ and $\mathbf{n}_R$ to the two tangent cones R_L and R_R would satisfy eqn (9), giving us eqn (11).

$$A\mathbf{X}_f = 0 \quad \text{with} \quad A = \begin{bmatrix} \mathbf{s}^T\bar{R}_L \\ \mathbf{s}^T\bar{R}_R \end{bmatrix} \tag{11}$$

A is a 2×4 matrix, the (right) null space of which gives a one-parameter family of solutions for $\mathbf{X}_f$ as given in eqn (12). Here $\mathbf{X}_{f1}$ and $\mathbf{X}_{f2}$ are four element vectors and γ is a scalar parameter.

$$\mathbf{X}_f = \mathbf{X}_{f1} + \gamma\mathbf{X}_{f2} \tag{12}$$

Since the frontier points lie on the surface of the cones, eqn (12) has to satisfy eqn (1) which would yield a quadratic equation in γ. Solving for γ and substituting in eqn (12) gives the two frontier points.

Since the plane under consideration is tangent to the quadric, its projection on the image plane would be tangent to the projected conic (occluding contour). The point of contact of the conic and the tangent line is the projection of the frontier point. The epipole lies on this same tangent line because the tangent plane contains the camera center of the other camera as shown above. Hence, the tangents drawn from the epipole to the conics should correspond over the two images (same plane projected on the two image planes). That is, they should adhere to the epipolar geometry (Hartley and Zisserman, 2003). This is the epipolar tangency constraint that the conics have to satisfy. Figure 3 shows this relationship where $\mathbf{e}_L$ and $\mathbf{e}_R$ are the epipoles and $\mathbf{l}_{L1}$, $\mathbf{l}_{L2}$, $\mathbf{l}_{R1}$ and $\mathbf{l}_{R2}$ are the corresponding epipolar tangents.

It could be seen that, if the projected conics satisfy this constraint, the points obtained from substituting the values of γ to either cone would yield the same results. If not, they would essentially be different.

5.1.1 Conic Adjustment Algorithm

As mentioned above, if the projected conics do not satisfy the epipolar tangency constraints, we get different sets of values for the frontier points when substituting to the equations of the two cones. For the scope of our application, where the deviation is not large enough to warrant iterative optimization methods, we assume that the mean of the two sets gives a reasonable approximation.

Thus, we have two points in space that (we assume) lie on both contour generators and hence we know that they would be on the projected conic contours as well. Further they would be on the common tangent plane and hence the epipolar lines drawn through these projected points should be tangent to the conic as well. We use this property in the adjustment of the conics.

We need to find the conic that goes through the projected frontier points $\mathbf{p}_1$ and $\mathbf{p}_2$ while being tangent to the epipolar lines $\mathbf{l}_1$ and $\mathbf{l}_2$ at the same points. The tangents to the conic C can be written as shown in eqn (13), where α_i are scalars constants.

$$\begin{aligned} \alpha_1\mathbf{l}_1 &= C\mathbf{p}_1 \\ \alpha_2\mathbf{l}_2 &= C\mathbf{p}_2 \end{aligned} \tag{13}$$

By row scanning the conic matrix C, and using only its unique elements, we get a vector $\mathbf{c}$. Let the points and lines be represented by $\mathbf{p}_i = [p_{i1} \;\; p_{i2} \;\; p_{i3}]$ and $\mathbf{l}_i = [l_{i1} \;\; l_{i2} \;\; l_{i3}]$ respectively, with $i = 1, 2$. They

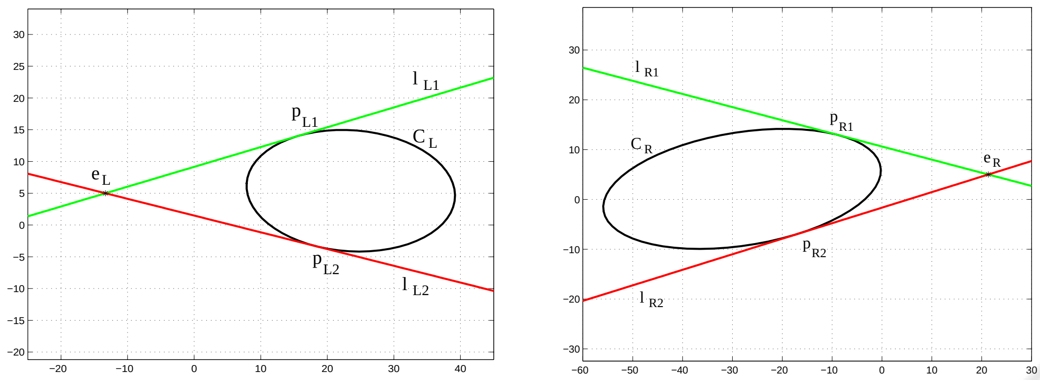

Figure 3: The Epipolar Tangency Constraints.

can then be represented in matrix form, P_i so that eqn (13) could be written as $\alpha_i \mathbf{l}_i = P_i \mathbf{c}$.

$$\mathbf{c} = [c_{11} \quad c_{12} \quad c_{13} \quad c_{22} \quad c_{23} \quad c_{33}]^T$$

$$P_i = \begin{bmatrix} p_{i1} & p_{i2} & p_{i3} & 0 & 0 & 0 \\ 0 & p_{i1} & 0 & p_{i2} & p_{i3} & 0 \\ 0 & 0 & p_{i1} & 0 & p_{i2} & p_{i3} \end{bmatrix}$$

Then, we can rewrite eqn (13) in the following form, with $\bar{\alpha}_i = -\alpha_i$.

$$N\mathbf{u} = 0$$

Where,

$$N = \begin{bmatrix} P_1 & \mathbf{l_1} & 0 \\ P_2 & 0 & \mathbf{l_2} \end{bmatrix} \quad \text{and} \quad \mathbf{u} = \begin{bmatrix} \mathbf{c} \\ \bar{\alpha}_1 \\ \bar{\alpha}_2 \end{bmatrix}$$

N is a 6×8 matrix of rank 6. Solving for the null space of N, we get a one-parameter family of vectors. By considering only the elements related to $\mathbf{c}$, we get the unique elements of this conic family. Here, $\mathbf{c_1}$ and $\mathbf{c_2}$ are 6 element vectors and β is a scalar parameter.

$$\mathbf{c} = \mathbf{c_1} + \beta \mathbf{c_2}$$

By rearranging the vector $\mathbf{c}$ to get the matrix form of C, we get the family of conics that satisfy the epipolar tangency constraints.

$$C = C_1 + \beta C_2 \tag{14}$$

The next step is to select the conic from this family that suits the fitted conic best. For this, from the equation of the fitted conic, we generate a set of points $\mathbf{x}_i = [x_i \quad y_i \quad 1]$ where $\mathbf{x}_i$ is the i^{th} point. We can also use the set of edge points in this calculation instead of points generated from the fitted conic. Let the number of points generated be n. First, we calculate the algebraic distance $d_i = \mathbf{x}_i^T C \mathbf{x}_i$ of each point from the family of conics C. From eqn (14), we get:

$$d_i = a_i + \beta b_i$$

Where,

$$a_i = \mathbf{x}_i^T C_1 \mathbf{x}_i \quad \text{and} \quad b_i = \mathbf{x}_i^T C_2 \mathbf{x}_i$$

The error e is defined as the sum of squares of algebraic distances for all points $\mathbf{x}_i$.

$$e = \sum_{i=1}^{n} d_i^2 = \sum_{i=1}^{n} a_i^2 + 2\beta \sum_{i=1}^{n} a_i b_i + \beta^2 \sum_{i=1}^{n} b_i^2$$

We need to find the value of the parameter β that minimizes the error e. Hence, the following has to be satisfied.

$$\frac{\partial e}{\partial \beta} = 2(\sum_{i=1}^{n} a_i b_i + \beta \sum_{i=1}^{n} b_i^2) = 0$$

This gives us the value for β that can be plugged into eqn (14) to get the best adjusted conic.

$$\beta = -\frac{\sum_{i=1}^{n} a_i b_i}{\sum_{i=1}^{n} b_i^2} \tag{15}$$

By applying this to both projected conics, we get a pair of conics that adhere to the epipolar tangency constraints. They also ensure that the adjusted conics are as close to the originally fitted conics as possible.

6 EXAMPLE APPLICATION

We apply our algorithm to data from a real-life application: namely fruit sorting. Here the fruits are placed on rollers whose dimensions and orientation in space are known. Each fruit rests on four conic rollers and images are captured by two cameras placed on either side of the rollers. Images taken from the two cameras

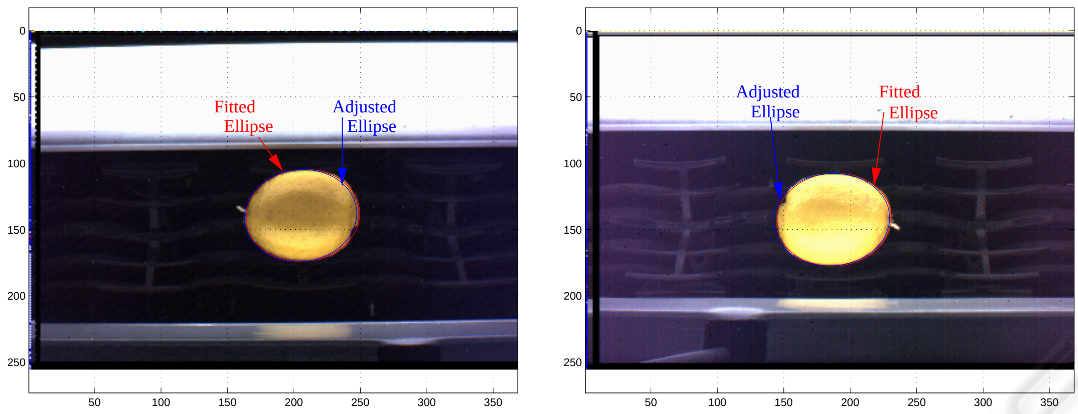

Figure 4: Images captured by two cameras with the fitted and adjusted conics.

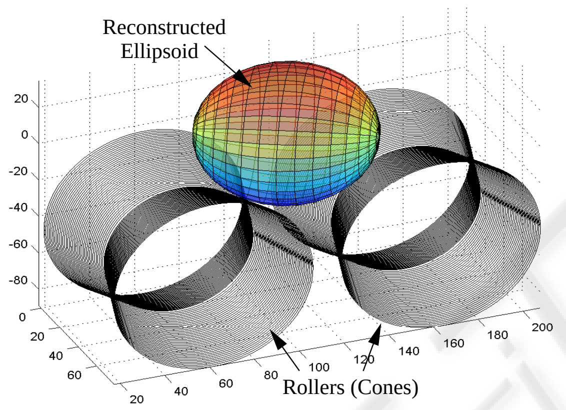

Figure 5: Reconstructed Ellipsoid.

along with the fitted and adjusted conics are shown in figure 4.

The roller information and the adjusted conics are then used to reconstruct the quadric as explained in section 3. Such a reconstructed quadric is shown in figure 5.

6.1 Error Analysis

For the analysis of error, we use two measures: re-projection error and volume error. The re-projection error by itself is not a full measure of the error involved. Any quadric selected from the family of quadrics reconstructed using eqn (5) would be projected on the image plane as the same conic. Hence, the error that is calculated by comparing the re-projection and the original fitted conic (or edge points) would just give a measure of the error involved in conic fitting and adjustment.

Hence, to get a true feel for the reconstruction error, we need to introduce another measurement. This is done by comparing the dimensions of the actual ellipsoid with its reconstructed counter-part. By calculating the volume of the actual and reconstructed ellipsoids, we obtain this second error measure, which along with the re-projection error gives a more rounded view of the reconstruction error.

For this experiment, we used spheres and ellipsoids of different dimensions and placed them at different positions and orientations. Then we calculated the re-projection and volume errors.

The re-projection error was measured as the normalized sum of squares of algebraic distances from the fitted conic to the re-projected conic. For n points on the fitted conic (or edge points), we calculate the error as given in eqn (16).

$$e_{rep} = \frac{1}{n}\sum_{i=1}^{n} d_i^2 \tag{16}$$

Where, d_i is the algebraic distance from the i^{th} point to the re-projected conic.

The volume error was calculated as the percentage error between the volumes of the actual and reconstructed ellipsoids. The results are summarized in table 1. The re-projection error indicates the mean of the errors calculated for the left and right images.

7 CONCLUSION

We proposed an algorithm for reconstructing ellipsoids given two occluding contours of views obtained from non-concentric cameras. First we adjusted the conics using a simple calculation as a prerequisite to the quadric fitting. Then, we discussed how the method introduced in (Cross and Zisserman, 1998)

Table 1: Error Analysis.

	Re-projection Error(10^{-5})	*Volume Error(%)*
Sphere 1	0.0563	3.1084
Sphere 2	2.0596	3.3040
Sphere 3	2.5063	2.6390
Ellipsoid 1	1.5880	3.4664
Ellipsoid 2	1.3303	3.1677
Ellipsoid 3	1.4047	3.2808
Ellipsoid 4	1.0186	4.8704

could be used to construct a family of quadrics in dual space. Then we use additional application specific information so that a unique quadric can be obtained.

The basic advantage of the proposed algorithm is that it avoids non-linear calculations. This is particularly important in the type of application this is aimed for. As shown in section 6.1, the errors involved are quite acceptable and part of that could be contributed to human errors involved in the obtaining of experimental measurements.

The drawback in this method is that the additional quadric surface(s), which the quadric to be reconstructed is tangent to, must be known. This may not be possible in some situations, making the algorithm unsuitable. Further, the errors in the measurements (for example, the distance of the known quadric from the origin of the world coordinate system), account for a large percentage of the reconstruction error. This makes the reconstruction sensitive to human errors.

Future work related to this research is to incorporate forward movement and rotation of the quadrics and to model the motion as well as the shape, location and orientation. Another avenue of research would be to come up with more accurate representations of the surfaces and to include texture information as well.

ACKNOWLEDGEMENTS

The authors would like to thank Mr. G.C. De Silva of Tokyo University, Japan for his invaluable input.

REFERENCES

Bruce, J. W. (1992). Lines, surfaces and duality. *Mathematical Proceedings of the Cambridge Philosophical Society*, 112:53–61.

Collins, S., Kozera, R., and Noakes, L. (2004). Shape recovery of a strictly convex solid from n-views. In *2nd International Conference on Computer Vision and Graphics*, pages 57–65, Warsaw, Poland.

Cross, G. (2000). *Surface Reconstruction from Image Sequences: Texture and Apparent Contour Constraints*. PhD thesis, University of Oxford.

Cross, G., Fitzgibbon, A. W., and Zisserman, A. (1999). Parallax geometry of smooth surfaces in multiple views. In *7th International Conference on Computer Vision*, pages 323–329, Kerkyra, Greece.

Cross, G. and Zisserman, A. (1998). Quadric reconstuction from dual-space geometry. In *6th International Conference on Computer Vision*, pages 25–31, Bombay, India.

Giblin, P. and Weiss, R. (1987). Reconstruction of surfaces from profiles. In *1st International Conference on Computer Vision*, pages 136–144, London, England.

Hartley, R. and Zisserman, A. (2003). *Multiple View Geometry in Computer Vision*. Cambridge University Press.

Kang, K., Tarel, J.-P., and Cooper, D. (2003). A unified linear fitting approach for singular and non-singular 3d quadrics from occluding contours. In *1st International Workshop on Higher-Level Knowledge in 3D Modeling and Motion Analysis*, Nice, France.

Kang, K., Tarel, J.-P., Fishman, R., and Cooper, D. (2001). A linear dual-space approach to 3d reconstruction from occluding contours using algebraic surfaces. In *8th International Conference on Computer Vision*, pages 136–144, Vancouver, Canada.

Karl, W. C., Verghese, G. C., and Willsky, A. S. (1994). Reconstructing ellipsoids from projections. *CVGIP: Graphical Model and Image Processing*, 56(2):124–139.

Ma, S. and Chen, X. (1994). Quadric surface reconstruction from its occluding contours. In *12th International Conference on Pattern Recognition*, pages 27–31, Jerusalem, Israel.

Ma, S. and Li, L. (1996). Ellipsoid reconstruction from three perspective views. In *13th International Conference on Pattern Recognition*, pages 344–348, Vienna, Austria.

Mendonca, P. R. S., Wong, K.-Y. K., and Cipolla, R. (2000). Camera pose estimation and reconstruction from image profiles under circular motion. In *6th European Conference on Computer Vision*, pages 864–877, Dublin, Ireland.

Porril, J. and Pollard, S. (1991). Curve matching and stereo calibration. *Image and Vision Computing*, 9(1):45–50.

Rieger, J. (1986). Three dimensional motion from fixed points of a deforming profile curve. *Optics Letters*, 11(3):123–125.

Wijewickrema, S. N. R. and Papliński, A. P. (2005). Principal component analysis for the approximation of an image as an ellipse. In *Proceedings of the 13th Conference in Central Europe on Computer Graphics and Visualization*, pages 69–70, Plzen, Czech Republic.